ELSEVIER

Thin Solid Films 294 (1997) 330–335

thin solid films

IR studies of p-type Si/SiGe quantum wells: intersubband absorption, IR detectors, and second-harmonic generation

M. Helm [a,*], P. Kruck [a], T. Fromherz [a], A. Weichselbaum [a], M. Seto [a], G. Bauer [a], Z. Moussa [b], P. Boucaud [b], F.H. Julien [b], J.-M. Lourtioz [b], J.F. Nützel [c], G. Abstreiter [c]

[a] *Institut für Halbleiterphysik, Universität Linz, A-4040 Linz, Austria*
[b] *Institut d'Electronique Fondamentale, Université Paris XI, F-91405 Orsay, France*
[c] *Walter Schottky Institut, TU München, D-85748 Garching, Germany*

Abstract

A survey is given of a variety of IR spectroscopy studies on p-type Si/SiGe quantum wells. Valence-band intersubband absorption experiments were performed on a large number of samples with different parameters and explained quantitatively by a self-consistent Luttinger–Kohn-type calculation. The dependence on polarization of the absorption was analyzed. On the basis of these quantum wells, mid-IR detectors were fabricated and characterized in terms of responsivity, dark current and detectivity. In asymmetric, compositionally stepped quantum wells, second-harmonic generation of CO_2 laser radiation was observed.

Keywords: IR study; Quantum wells; Silicon; Germanium

1. Introduction

The resonant interaction of IR radiation with quantized energy levels in semiconductor quantum wells (QWs) has been studied in many material systems over the past decade [1]. Applications from IR lasers [2] to detectors [3] and non-linear optical effects [4,5] have been reported. Owing to the great progress in epitaxial growth techniques, such investigations have also become possible for Si/SiGe structures. In particular, p-type SiGe quantum wells have turned out to be most promising, since they can be grown pseudomorphically on Si substrates. In this case most of the band offset occurs in the valence band. In contrast, n-type Si/SiGe quantum wells require the growth of a thick, graded SiGe buffer layer in order to obtain a finite conduction band offset.

In the present paper we discuss the general features of intersubband absorption in p-type Si/SiGe quantum wells and present experimental data on a series of samples with different parameters. As an application we describe the realization of an Si/SiGe quantum well IR photodetector (QWIP) and its performance. Finally we present some results on a non-linear optical process, the IR second-harmonic generation in an asymmetric, compositionally stepped quantum well structure.

* Corresponding author. Tel: +43-70-2468-9602; Fax: +43-70-2468-650; E-mail: m.helm@hlphys.uni-linz.ac.at

PII S0040-6090(96)09214-0

2. General considerations

The conceptually simplest possible semiconductor quantum well structure is achieved by confining electrons at the Γ-point. Owing to the symmetry and the simplicity of the band structure, in this case intersubband transitions are only allowed for radiation containing a polarization component along the growth axis (z-direction). In order to couple the IR radiation to the electronic transition, a multipass waveguide geometry is frequently employed, where the light is coupled into the sample at a wedged facet and subsequently undergoes several total internal reflections [6]. The s-polarization contains only an electric-field component in the layer planes (xy direction), whereas the p-polarization contains both xy and z components and, therefore, couples to the intersubband transition. In addition, if the active multiquantum well (MQW) layer is close to the sample surface and its thickness is much smaller than the resonant wavelength of the radiation, the electromagnetic boundary conditions require a metal layer to be deposited onto the sample surface in order to make the z polarized transitions observable [7].

For p-type quantum wells the situation is more complex. Owing to the coupling of heavy-hole (HH), light-hole (LH), and spin-orbit split-off (SO) bands, some transitions are also allowed for xy-polarized radiation [8–15]. This is why p-

type quantum wells are well suited for normal-incidence IR detectors [13–15].

3. Samples

All the investigated samples were grown by molecular beam epitaxy (MBE) in a commercial chamber (Riber SIVA 32) at the Walter Schottky Institute on n-type ($\rho = 1500$ Ω cm) Si(001) substrates. They typically consist of 10–30 periods of $Si_{1-x}Ge_x$ quantum wells with a thickness of 20–70 Å and a Ge content of 20%–60%. The thickness of the Si barrier varies between 150 Å and 500 Å. Boron doping was introduced either into the barriers (modulation doping) or into the wells, resulting in areal hole densities of $(0.4–3) \times 10^{12}$ cm^{-2} per quantum well. Routine characterization was performed by high-resolution triple-axis X-ray diffraction and reciprocal space mapping [16].

4. Intersubband absorption

Intersubband absorption in quantum wells was first reported by West and Eglash [17] in n-type GaAs, and later on in many other material systems, both n- and p-type. Hole intersubband absorption in SiGe quantum wells has been observed by several groups [12,13,15,18–20], initially on very highly doped structures [13], where the absorption spectra were dominated by free-carrier [18] and plasma [12] effects. Only recently has a coherent picture emerged of the various transitions involved in the absorption process.

The intersubband absorption experiments were performed with a Bruker Fourier transform spectrometer (FTS). The samples were prepared in the waveguide geometry discussed above with a metal layer deposited on top and were placed in a liquid-He flow cryostat. Most measurements were performed at $T = 10$ K.

Fig. 1 shows absorption spectra of several quantum well samples obtained by dividing the p-polarized transmission by the s-polarized transmission, and further normalized to the same transmission ratio of an undoped Si substrate prepared in the same manner. Any possible s-polarized absorption is shorted out by the metal layer on the surface. The experimental spectra are represented by the solid lines.

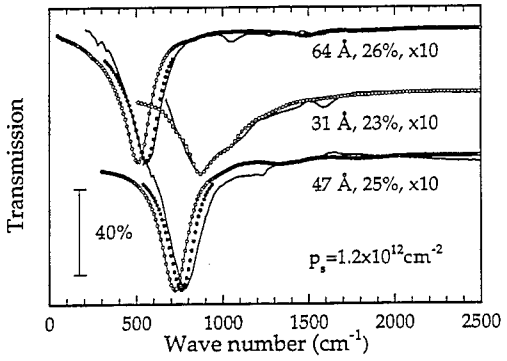

Fig. 1. Transmission spectra ($T = 10$ K) of three modulation doped Si/SiGe MQWs with a Ge content of approximately 25% and various well widths as indicated: ——— experiment, ○ theory without depolarization shift, ● theory with depolarization shift (for details see text).

In order to understand the position and the shape of the absorption lines, we performed a self-consistent six-band Luttinger–Kohn type envelope function calculation [20], which takes into account the band bending due to charge transfer, the exchange-correlation correction within the local density approximation, the strain in the quantum well, and the in-plane dispersion of the subbands. The resulting band structure was used as an input for a dielectric simulation of the waveguide structure [20] (including the multilayer stack and the electromagnetic boundary conditions). The results of this calculation are plotted as the open symbols in Fig. 1. For the two widest quantum wells the depolarization shift [21] also turns out to be significant and was calculated in a one-band model. The final result is represented by the full symbols. For all the narrower QWs, whose main intersubband absorption occurs at higher energies, the depolarization shift is a negligible correction. The main conclusions from the calculation are as follows [20]. For most samples the strong absorption line is due to the HH1–HH2 intersubband transition and follows the usual intersubband selection rule, i.e. it is only allowed for z-polarized radiation. In the sample with 31 Å well width and 23% Ge content, the HH2 level is localized in the barriers and the absorption goes to the HH3, HH4 and HH5 states, which are located very close to each other and are actually miniband states in the continuum. This is why the absorption line is quite broad and shows some fine structure on the high-energy side. A similar situation occurs for the very narrow wells (22–23 Å) with large Ge content (Fig. 2). Here, however, some additional line broadening has to be assumed owing to the diminished material quality at these high Ge contents ($x > 50\%$). We would like to point out that the only fitting parameters in the calculation are a single line broadening parameter and a correction factor for the absolute magnitude of the absorption, which is between 0.5 and 1 for each sample. This is not surprising, since the hole concentrations are not known very accurately. The above samples are relatively low doped (less than or equal to 1.2×10^{12} cm^{-2}), resulting in a typical Fermi energy of only

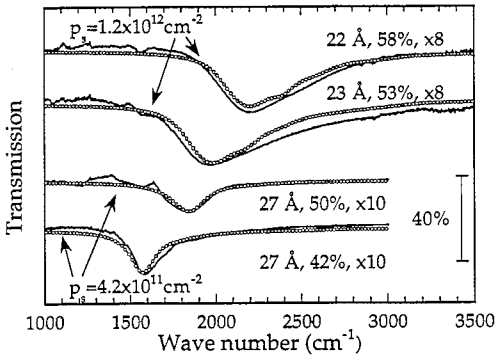

Fig. 2. Same as Fig. 1, for MQWs with higher Ge content and narrower wells.

10 meV. As a consequence, the observed absorption lines are quite narrow, since only k-values near zero participate in the absorption. For the same reason xy-polarized transitions cannot be observed in these samples (even when there is no metal layer on the surface); calculations show that most of these transitions become significant only at much larger k-values.

Therefore another sample was grown in order to study the dependence on polarization of the absorption. It consisted of 30 $Si/Si_{0.71}Ge_{0.29}$ quantum wells of 30 Å thickness, separated by 150 Å wide Si barriers. The p-type (modulation) doping was increased to 2.8×10^{12} cm^{-2}. In addition, a 1.25 μm undoped Si cap layer was grown on top. Because of this setback of the MQW sequence from the surface and the large number of 30 periods, both polarization components couple effectively to the respective transitions and the dependence on polarization of the absorption can be investigated on the same sample [22].

The results are shown in Fig. 3 by the solid lines. Here the p-(s-)polarized sample transmission is normalized by the p-(s-)polarized transmission of an undoped Si substrate. The s-polarized spectrum shows a narrow absorption line at 400 cm^{-1} and a broad feature between 1200 and 2500 cm^{-1}, which can be remarkably well reproduced by the calculations (lines with open symbols). Detailed analysis of the band structure shows [22] that the line at 400 cm^{-1} corresponds to the HH1–LH1 transition, which is allowed only for $k\neq0$. The broad absorption band consists of the HH1–SO2 transition (between 1800 and 2400 cm^{-1}) and a transition to a subband which has a mixed HH–LH–SO character (1200–1800 cm^{-1}), the latter again only at $k\neq0$. All the final states of the broad absorption feature are continuum bands well above the barriers. The p-polarized spectrum shows a strong line at 1000 cm^{-1}, which can be identified as the 'usual' HH1–HH2 intersubband transition. In order to understand the additional features, one must keep in mind that the p-polarization contains both z and xy components of the electric field, so these features are the same as in the s-polarized spectrum. Finally note that the data between 550 and 650 cm^{-1} are very noisy (and therefore not shown), and that the experimental spectra contain a background which can mostly be ascribed to free-carrier absorption [18].

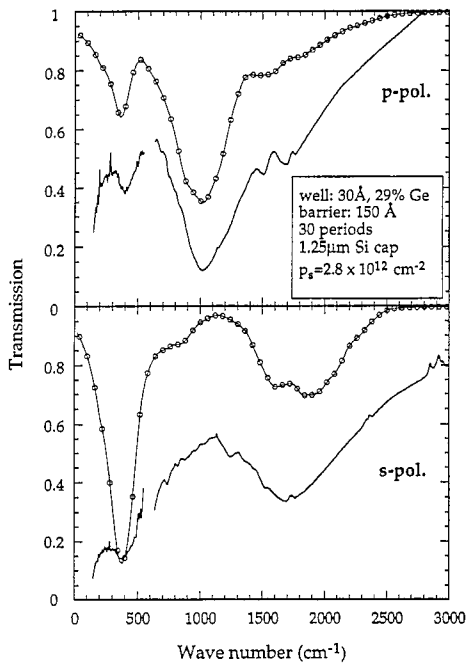

Fig. 3. Polarization dependent transmission spectrum (at $T=10$ K) of an Si/SiGe MQW with parameters as indicated: ——— experiment, O———O calculation. Note that the s-polarization contains only xy electric-field components, whereas the p-polarization contains both z and xy components.

5. IR detectors

Efforts for the development of IR detectors based on quantum wells were started to provide an alternative for the most frequently employed HgCdTe. Many investigations focused on GaAs based devices [3], but recently also SiGe QWIPs have been reported [15], which have the advantage of being compatible with standard Si technology and electronics. An SiGe based QWIP structure utilizes transitions from the ground state (HH1) to excited states which are close to or above the barriers, so the photo-excited holes can give rise to a photocurrent [3]. Furthermore the Si barriers have to be thick in order to minimize the dark current (i.e. make the tunneling contribution to the dark current negligible) and the MQW layers have to be enclosed between heavily doped p-type contacts. For recent volumes on QWIPs (Si/SiGe and others) see Ref. [23].

The detector structure presented here [24] consists of 10 periods of 30 Å thick $Si/Si_{0.65}Ge_{0.35}$ quantum wells which are separated by 500 Å thick Si barriers. For detector structures it appears more appropriate to introduce the doping directly into the quantum wells (1.5×10^{12} cm^{-2} in the present case), since modulation doping would lead to band bending and thus to an effective decrease in the barrier width and height. Also photo-excited carriers could become trapped in the barriers.

The samples were processed into 200 μm × 200 μm square mesas by reactive ion etching. Standard metallization was applied to the contact layers. The photoresponse measurements were performed both under direct normal incidence and by coupling through a wedged facet. The latter geometry allows one to analyze the dependence on polarization. Fig. 4 shows the results of these measurements at $T=77$ K. A peak responsivity of 50 mA W^{-1} is observed at a wavelength of $\lambda_p=5$ μm and a bias voltage of $V_b=3$ V (increasing to 75 mA W^{-1} at $V_b=4$ V), a value comparable with p-type GaAs QWIPs [14], but smaller than for n-type GaAs QWIPs [3]. Quite surprisingly, the response is higher in s-polarization than in p-polarization [25], which is in contrast to the transmission results on similar samples. A reason for this may be the influence of the final state in the absorption process on

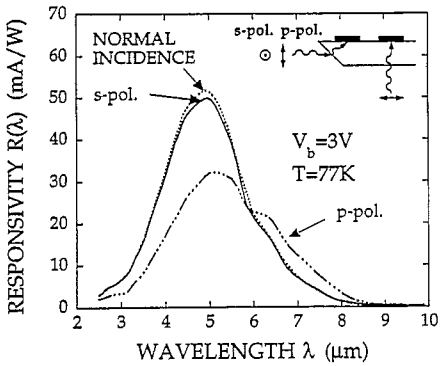

Fig. 4. Spectral photoresponse of the Si/SiGe detector (at $T=77$ K) for a bias voltage of $V_b=3$ V. Shown are the spectra taken at normal incidence, with s-polarization, and p-polarization. The corresponding experimental geometries are shown in the inset.

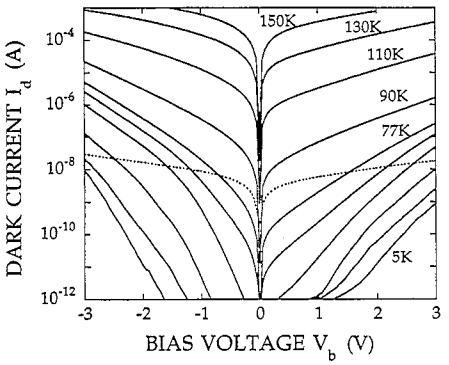

Fig. 5. Detector dark current as a function of bias voltage for temperatures $T=5$, 10, 30, 50, 70, 77, 90, 110, 130, and 150 K. The dashed line is the photocurrent generated by the room-temperature background radiation entering through the dewar window.

the photo-excited carrier transport [26]. z-polarized radiation excites holes mainly into the HH2 state, whereas xy polarized radiation excites them into the LH and SO states; since the latter are higher in energy and have a smaller effective mass, transport may be more efficient here. Also note that the p-polarized spectrum contains both z and xy electric field components. This is why the spectral shape for s- and p-polarization is quite similar except for the long-wavelength cut-off, where the p absorption is dominated by the HH1–HH2 transition.

For further characterization the dark current was measured as a function of temperature, which is shown in Fig. 5. The dashed lines indicate the contribution of the 300 K background radiation to the photocurrent. From the intersection points it can be concluded that background limited performance (BLIP) is achieved at temperatures as high as 85 K for $V_b=0.8$ V. Combining the responsivity and dark current results we obtain a detectivity of $D^*=2\times10^{10}$ cm $Hz^{1/2}$ W^{-1} at $T=77$ K and $V_b=0.8$ V. At higher bias D^* of course drops owing to the increasing dark current. The activation energy which can be extracted from the dark-current curves agrees very well with the p-polarized cut-off wavelength [24].

6. Second-harmonic generation

Intersubband optical transitions cannot only be utilized for linear absorption processes, but also for non-linear optical phenomena. However, in order to make second-order non-linear processes possible, the inversion symmetry of the quantum well has to be broken. This can be done by growing asymmetric coupled quantum wells or compositionally stepped quantum wells, as has been demonstrated for several III–V semiconductor systems [4,5]. We have used the latter type to investigate the frequency doubling of 10.6 μm CO_2 laser radiation. The Si/SiGe system is different from the III–V systems, since the substrate is inversion symmetric and does not posses a second-order non-linear susceptibility.

The sample consisted of 15 stepped quantum wells with 36 Å $Si_{0.75}Ge_{0.25}$, 19 Å $Si_{0.57}Ge_{0.43}$, separated by 200 Å Si barriers. The doping was placed in the quantum wells with an areal hole concentration of $p=2.2\times10^{12}$ cm^{-2}. This structure is designed in a way that the HH1, HH2 and HH3 levels are separated by approximately 120 meV each, the photon energy of the CO_2 laser. Thus the non-linear susceptibility responsible for second-harmonic generation (SHG) can be expected to be enhanced owing to the near-resonant conditions.

First the linear absorption was measured in a similar way as described in Section 1 (Fig. 6). A strong absorption peak is observed at approximately 150 meV, which can be assigned to the HH1–HH2 transition. The shoulder visible at approximately 230 meV is due to the HH1–HH3 transition, which is allowed because of the broken symmetry. The relative strength of the two absorption lines compares reasonably well with the calculation, which yields a 3:1 ratio for the HH1–HH2 and HH1–HH3 oscillator strengths respectively. The absolute line positions deviate somewhat from the theoretical values; this can be ascribed to a deviation of the actual sample parameters from the nominal values (owing to the complicated layer structure, X-ray analysis does not permit a unique

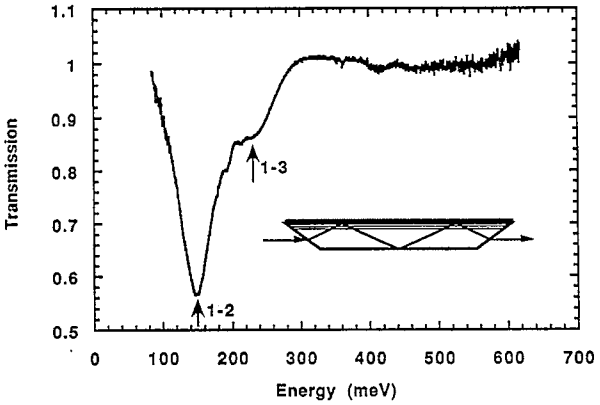

Fig. 6. Transmission spectrum of the compositionally stepped Si/SiGe MQW structure recorded at $T=10$ K. The HH1–HH2 and HH1–HH3 transitions are indicated.

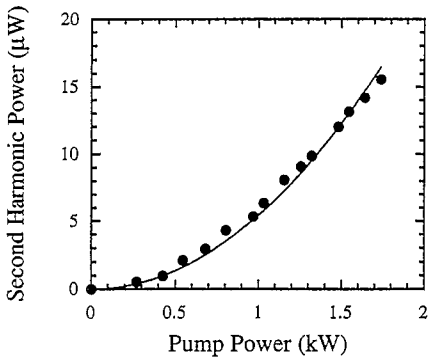

Fig. 7. Second-harmonic power vs. input pump power. The solid line is a quadratic fit to the experimental points.

determination of the individual layer thicknesses and compositions).

The SHG experiment [27,28] was performed using a grating tunable, rotating-mirror Q-switched CO_2 laser yielding 150 ns pulses with a peak power of 2 kW. The radiation was focused onto the long edge of the rectangular shaped sample (focal spot 170 μm diameter) covered with a metal layer to enhance the coupling of the *z*-polarized radiation. A part of the laser was diverted into a pyroelectric detector and used as a power reference and a trigger signal. The frequency doubled signal after the sample was collected and focused with two ZnSe lenses into a liquid-nitrogen-cooled InSb detector. The transmitted 10 μm laser radiation was blocked using a sapphire window and a 5 μm band-pass filter, the latter to block all thermal radiation which might result from heating effects. Two polarizers before the sample were used to vary the laser power and a polarizer after the sample to analyze the polarization of the second-harmonic signal. The polarization of the incoming radiation could be rotated from vertical to horizontal with a $\lambda/2$ plate (only at 10.6 μm).

Fig. 7 shows the second-harmonic power as a function of input power recorded at room temperature. Both the pump beam and the SHG radiation were polarized along the growth axis, which implies that the (*zzz*) component of the non-linear optical susceptibility tensor $\chi^{(2)}$ is responsible for the SHG. A quantitative analysis of previous results obtained in Brewster-angle geometry [27] gave a numerical value of $\chi^{(2)}{}_{zzz} = 5 \times 10^{-8}$ m V^{-1}, in rough agreement with a theoretical estimate. In the present measurement a much better coupling efficiency is achieved; however, for a quantitative evaluation a mode propagation analysis appears to be necessary.

In a similar manner as *xy* polarized absorption can be observed in p-type quantum wells, also other $\chi^{(2)}$ components are expected to be finite, as has been demonstrated for p-GaAs quantum wells [29]. To clarify this issue for Si/SiGe quantum wells, more experimental work is required using different sample geometries.

7. Summary

We have attempted to show that owing to the matured Si/SiGe heteroepitaxial growth techniques and the resulting material quality it has become possible to study the resonant interaction of IR radiation with quantum-confined energy levels in this material system. Hence 'band-structure engineering' can be performed in Si/SiGe structures, much the same as is done in III–V semiconductors, although there will of course always be the restriction of the large lattice mismatch between Si and Ge. We have shown that a basic understanding of intersubband absorption can be obtained in Si/SiGe quantum wells and that this knowledge can be exploited for the development of devices such as IR detectors or for non-linear optical phenomena such as second-harmonic generation.

Acknowledgements

This work was supported by the FWF, the BMfWFK, and the GME (Austria).

References

[1] for a recent survey, see H.C. Liu, B.F. Levine and J.Y. Andersson (eds.), *Quantum Well Intersubband Transition Physics and Devices*, Kluwer, Dordrecht, 1993.
[2] J. Faist, F. Capasso, D.L. Sivco, C. Sirtori, A.L. Hutchinson and A.Y. Cho, *Science, 264* (1994) 553.
[3] B.F. Levine, *J. Appl. Phys., 74* (1993) R1.
[4] E. Rosencher and Ph. Bois, *Phys. Rev. B, 44* (1991) 11415.E. Rosencher, A. Fiore, B. Vinter, V. Berger, Ph. Bois and J. Nagle, *Science, 271* (1996) 168.
[5] F. Capasso, C. Sirtori and A.Y. Cho, *IEEE J. Quantum Electron., 30* (1994) 1313.
[6] H. Hertle, G. Schuberth, E. Gornik, G. Abstreiter and F. Schäffler, *Appl. Phys. Lett., 59* (1991) 2977.
[7] M.J. Kane, M.T. Emeny, N. Apsley, C.R. Whitehouse and D. Lee, *Semicond. Sci. Technol., 3* (1988) 722.
[8] Y.C. Chang and R.B. James, *Phys. Rev. B, 39* (1989) 12672.
[9] P. Man and D.S. Pan, *Appl. Phys. Lett., 61* (1992) 2799.
[10] E. Corbin, K.B. Wong and M. Jaros, *Phys. Rev. B, 50* (1994) 2339.
[11] F. Szmulowicz and G.J. Brown, *Phys. Rev. B, 51* (1995) 13203.
[12] S.K. Chun, D.S. Pan and K.L. Wang, *Phys. Rev. B, 47* (1993) 15638.
[13] J.S. Park, R.P.G. Karunasiri and K.L. Wang, *Appl. Phys. Lett., 61* (1992) 681.R.P.G. Karunasiri, J.S. Park and K.L. Wang, *Appl. Phys. Lett., 61* (1992) 2434.
[14] B.F. Levine, S.D. Gunapala, J.M. Kuo, S.S. Pei and S. Hui, *Appl. Phys. Lett., 59* (1991) 1864.
[15] R. People, J.C. Bean, C.G. Bethea, S.K. Sputz and L.J. Peticolas, *Appl. Phys. Lett., 61* (1992) 1122.
[16] G. Bauer, J. Li and E. Koppensteiner, *J. Cryst. Growth, 157* (1995) 61.
[17] L.C. West and S.J. Eglash, *Appl. Phys. Lett., 46* (1985) 1156.
[18] S. Zanier, J.M. Berroir, Y. Guldner, J.P. Vieren, I. Sagnes, F. Glowacki, Y. Campidelli and P.A. Badoz, *Phys. Rev. B, 51* (1995) 14311.
[19] P. Boucaud, L. Gao, Z. Moussa, F. Visocekas, F.H. Julien, J.-M. Lourtioz, I. Sagnes, Y. Campidelli and P.-A. Badoz, *Appl. Phys. Lett., 67* (1995) 2948.
[20] T. Fromherz, E. Koppensteiner, M. Helm, G. Bauer, J.F. Nützel and G. Abstreiter, *Phys. Rev. B, 50* (1994) 15073.T. Fromherz, E. Koppensteiner, M. Helm, G. Bauer, J.F. Nützel and G. Abstreiter, *Superlattice Microstruct., 15* (1994) 229.
[21] S.J. Allen, Jr., D.C. Tsui and B. Vinter, *Solid State Commun., 20* (1976) 425.T. Ando, *Solid State Commun., 21* (1977) 133.

[22] T. Fromherz, P. Kruck, M. Helm, G. Bauer, J.F. Nützel and G. Abstreiter, *Superlattice Microstruct., 20* (1996) 237.T. Fromherz, P. Kruck, M. Helm, G. Bauer, J.F. Nützel and G. Abstreiter, *Appl. Phys. Lett., 68* (1996) 3611.

[23] M.O. Manasreh (ed.), *Semiconductor Quantum Wells and Superlattices for Long-Wavelength Infrared Detectors*, Artech House, Boston, MA, 1993.M.H. Francombe and J.L. Vossen (eds.), *Homojunction and Quantum Well Infrared Detectors*, Academic Press, San Diego, CA, 1995.

[24] P. Kruck, A. Weichselbaum, M. Helm, T. Fromherz, G. Bauer, J.F. Nützel and G. Abstreiter, *Appl. Phys. Lett., 69* (1996) 3372.

[25] A. Fenigstein, E. Finkman, G. Bahir and S.E. Schacham, *J. Appl. Phys., 76* (1994) 1998.

[26] H.C. Liu, *Appl. Phys. Lett., 60* (1992) 1507.

[27] M. Seto, M. Helm, Z. Moussa, P. Boucaud, F.H. Julien, J.-M. Lourtioz, J.F. Nützel and G. Abstreiter, *Appl. Phys. Lett., 65* (1994) 2969.

[28] P. Kruck, M. Seto, M. Helm, Z. Moussa, P. Boucaud, F.H. Julien, J.-M. Lourtioz, J.F. Nützel and G. Abstreiter, *Solid State Electron., 40* (1996) 763

[29] M.J. Shaw, M. Jaros, Z. Xu, P.M. Fauchet, C.W. Rella, B.A. Richman, H.A. Schwettman and G.W. Wicks, *Phys. Rev. B, 50* (1994) 18395.